miRNA-101 Targets TGF-βR1 to Retard the Progression of Oral Squamous Cell Carcinoma

Yong Wang,* Rui-Zhi Jia,* Shu Diao,* Jun He,† and Li Jia†

*Department of Pediatric Dentistry, Beijing Stomatological Hospital & School of Stomatology,
Capital Medical University, Beijing, China
†Evaluation and Research Center for Toxicology, Institute of Disease Control and Prevention of PLA, Beijing, China

Despite the considerable knowledge on the involvement of microRNA-101 (miR-101) in the evolution of oral squamous cell carcinoma (OSCC), the underlying mechanisms remain obscure. In this study, miR-101 expression was markedly downregulated in the OSCC cell lines and tissues. Cell counting kit-8 (CCK-8), ethynyl deoxyuridine (EdU), and colony formation assays showed that miR-101 inhibited the proliferation of OSCC cells. Flow cytometry and caspase 3 activity assays indicated that miR-101 induced OSCC cell apoptosis. Transwell assays demonstrated that this miRNA also repressed OSCC cell migration and invasion. Moreover, tube formation assay showed that miR-101 abated the proangiogenesis of OSCC cells. Dual-luciferase reporter assay confirmed that miR-101 directly targeted transforming growth factor-β receptor 1 (TGF-βR1) in OSCC. Ectopic expression of TGF-βR1 counteracted the effects of miR-101 on the OSCC cell characteristics. Thus, miR-101 significantly abolished the proliferation, motility, and proangiogenesis of OSCC cells and induced their apoptosis by targeting TGF-βR1. These results imply the potential application of miR-101 in OSCC treatment.

Key words: miR-101; Transforming growth factor-β receptor 1 (TGF-βR1); Oral squamous cell carcinoma (OSCC); Growth; Metastasis

INTRODUCTION

Oral squamous cell carcinoma (OSCC) is a common type of cancer characterized by a low survival rate, primarily due to local recurrence and metastasis[1]. This malignancy accounts for more than 200,000 new cancer cases annually worldwide[2,3]. Despite remarkable advances in diagnosis and therapy, the 5-year survival rate of patients with OSCC remains below 50%[4,5]. Thus, identifying the pathogenesis of OSCC and novel therapeutic strategies is highly essential and imperative.

MicroRNAs (miRNAs) are a class of noncoding RNAs [21–23 nucleotides (nt)] that regulate gene expression[6]. miRNAs play key roles in various biological processes, such as cell differentiation, proliferation, and apoptosis[7–9]. Recent evidence has indicated that miRNAs are highly implicated in a series of human cancers, including OSCC[10–13]. Downregulated miRNA-101 (miR-101) acts as a tumor suppressor in several cancer types[14–23]. The ERK2-ZEB1/miR-101 axis contributes to epithelial–mesenchymal transition and motility of cancer cells[16].

Enhanced miR-101 suppresses colony formation and invasion of colorectal cancer cells[19]. miR-101 hinders the proliferation and induces apoptosis by targeting the EYA transcriptional coactivator and phosphatase 1 in breast cancer[23]. Previously, we have also paid close attention to the roles of miRNA-101 in cancers and have performed miRNA-101-related experiments in several types of cancers, including OSCC. Moreover, the expression and biological roles of miR-101 in OSCC remain unclear. Thus, in the present study, we chose miRNA-101 as the research objective in OSCC.

In this study, we investigated the expression and biological functions of miR-101 in OSCC and found that miR-101 levels were dramatically downregulated in OSCC cell lines and tissues. Dual-luciferase reporter assays revealed that miR-101 directly targeted transforming growth factor-β receptor 1 (TGF-βR1). miR-101 significantly repressed proliferation and motility but promoted cell apoptosis, which was counteracted by the rescue of TGF-βR1. These results provided novel insights into the molecular mechanisms by which miR-101

Address correspondence to Li Jia, Evaluation and Research Center for Toxicology, Institute of Disease Control and Prevention of PLA, 27 Taiping Road, Hai Dian District, Beijing 100071, China. Tel: +(86)-10-68218213; Fax: +(86)-10-68218213; E-mail: lijiacdc@163.com

reduced OSCC growth and metastasis. Thus, miR-101 is a promising therapeutic agent for OSCC.

MATERIALS AND METHODS

Cell Culture

Human normal oral keratinocytes (hNOKs) were purchased from ScienCell Research Laboratories (Carlsbad, CA, USA) and cultured in an oral keratinocyte medium (ScienCell Research Laboratories). Human OSCC cell lines, including Tca8113, OSCC-15, SCC-9, and SCC-25, were obtained from the American Type Culture Collection (Manassas, VA, USA). All cells were used no later than 6 months after they were received. OSCC cells were cultured in Dulbecco's modified Eagle's medium (DMEM)/Nutrient Mixture F12 (Gibco, Carlsbad, CA, USA) supplemented with 10% fetal bovine serum (FBS; Gibco), 2 mM L-glutamine, and 100 µg/ml penicillin/streptomycin (Sigma-Aldrich, St. Louis, MO, USA) in a humidified incubator containing 5% CO_2 at 37°C. The cells from passage 4 were prepared for the experiments. Recombinant human TGF-β1 (Sigma-Aldrich) was used at a final concentration of 2 ng/ml. Other reagents were procured from Sigma-Aldrich unless otherwise stated.

Cell Transfection

miR-101 and miR-NC (negative control) mimics were synthesized by RiboBio (Guangzhou, China). Lipofectamine 2000 reagent (Invitrogen, Carlsbad, CA, USA) was purchased for cell transfection, which was performed according to the manufacturer's instructions. When cell confluence reached 80%, 80 nM miR-101 or miR-NC mimics were transfected into the SCC-9 and Tca8113 cells (1×10^6 cells/6-cm dish).

Dual-Luciferase Reporter Assay

Plasmid pGL3-TGF-βR1-3′-UTR-WT or pGL3-TGF-βR1-3′-UTR-MUT was obtained from Biovector (Beijing, China) and cotransfected with miR-101 or miR-NC mimics into OSCC cells. A luciferase assay was conducted 48 h after transfection using a dual-luciferase reporter assay kit (Promega, Madison, WI, USA). *Renilla* luciferase was cotransfected as a control for normalization.

Cell Proliferation Assay

Cell viability was detected by ethynyl deoxyuridine (EdU) incorporation assay. The cells seeded in a 96-well plate (1×10^3 cells/well) were transfected with miR-101 mimics, miR-NC, or miR-101 mimic + TGF-βR1-expressing plasmid. At 48 h after transfection, EdU incorporation assays were performed with a commercial kit (RiboBio) following the manufacturer's protocol. Six random fields of each well were selected to observe and photograph under an inverted fluorescence microscope (Carl-Zeiss, Berlin, Germany).

Colony Formation Assay

A total of 1×10^3 SCC-9 or Tca8113 cells were cultivated in 3-cm plates precoated with 1% agar (Sigma-Aldrich). At 48 h after transfection, fresh culture medium was replaced, and the treated cells were cultured for another 12 days. The cells were fixed with methanol, and the colonies were stained with 0.4% crystal violet (Sigma-Aldrich) and counted under a microscope (Olympus, Tokyo, Japan). Five random fields were selected for each well to determine the total number of colonies.

Quantitative Real-Time Polymerase Chain Reaction (qPCR) Assay

For RNA extraction, the fresh tissues and cells were lysed using TRIzol reagent (Invitrogen) and purified using RNeasy Mini Kit (Qiagen, Valencia, CA, USA). Complementary DNA was synthesized using reverse transcriptase (Epicentre, Madison, WI, USA) or the miS-cript Reverse Transcription Kit (Qiagen) and then amplified using SYBR Premix Ex Taq™ (TaKaRa, Otsu, Shiga, Japan). The mRNA and miRNA levels were determined by the $2^{-\Delta\Delta Ct}$ method, with glyceraldehyde-3-phosphate dehydrogenase (GAPDH) and U6 as internal controls, respectively. The primers used for PCR amplification were as follows: for TGF-βR1, 5′-ACTGGCAGCTGTCATTGCTG GACCAG-3′ (forward) and 5′-CTGAGCCAGAACCTGACGTTGTCATATCA-3′ (reverse); for GAPDH, 5′-TGCACCACCAACTGC TTAGC-3′ (forward) and 5′-GGC ATGGACTG TGGTC ATGAG-3′ (reverse); for miR-101, 5′-CGGCGGTAC AGTACT GTGATAA-3′ (forward) and 5′-CTGGTGTC GTGGAGTCGGCAATTC-3′ (reverse); and for U6, 5′-CTCGCTTCGGCAGCACA-3′ (forward) and 5′-AAC GCTTCACGA ATTT GCGT-3′ (reverse).

Quantitative Caspase 3 Activity Assay

Caspase 3 activity assay was conducted using the Caspase 3/CPP32 Colorimetric Assay Kit (Biovision, Palo Alto, CA) according to the standard protocols. SCC-9 and Tca8113 cells were cotransfected with RNA oligonucleotides and with or without plasmids for 48 h. The cells were harvested, washed with cold phosphate-buffered saline (PBS), and lysed using chilled lysis buffer for 10 min. After centrifugation at $10,000 \times g$, protein (150 µg) was added into 2×50 µl of reaction buffer containing 5 µl of *N*-acetyl-Asp-Glu-Val-AsppNA substrate (200 µM; final concentration). After incubation for 2 h at room temperature, *N*-acetyl-Asp-Glu-Val-Asp-pNA cleavage was monitored using a microplate reader (Bio-Tek Instruments Inc., Winooski, VT, USA). The absorbance

(405 nm) of each well was detected to evaluate enzyme-catalyzed pNA release.

Flow Cytometry Assay

SCC-9 and Tca8113 cells were seeded into six-well plates and transfected with RNA oligonucleotides for 48 h. Cell apoptosis was determined using annexin V fluorescein isothiocyanate (FITC) and propidium iodide (PI) staining assay. After the OSCC cells were harvested and resuspended in PBS, 10 μl of ready-to-use annexin V-FITC (BD Bioscience, San Jose, CA, USA) was added into the mixture. The cells were incubated at 37°C for 15 min and counterstained with 5 μl of PI in the dark for 30 min. The fluorescence was assessed by using a BD FACSCalibur flow cytometer (BD Bioscience), and the results were analyzed using CellQuest software (BD Bioscience).

Migration and Invasion Assays

Cell motility assay was performed using Transwell chambers (8-μm pore size; BD Biosciences). For the migration assay, after transfection with miR-101 mimics, miR-NC, or miR-101 mimic + TGF-βR1-expressing plasmid for 48 h, 3×10^4 cells were seeded into the upper chamber with serum-free medium. An invasion assay was performed using a Transwell system (8-μm pore size, Matrigel-coated polycarbonate membrane; BD Biosciences). Subsequently, 5×10^4 transfected cells were plated into the upper chambers with serum-free medium. A complete medium containing 100 ng/ml TGF-β1 (Sigma-Aldrich) was added to the lower chamber as a chemoattractant. After incubation for 24 h at 37°C, a cotton swab was utilized to scrape and remove the cells from the upper surface of the membrane. The migrated and invaded cells were stained with 0.4% crystal violet, visualized, and counted in five separate fields per membrane under an inverted microscope (Olympus).

Protein Extraction and Western Blot Analysis

After OSCC cells were treated with miR-NC or miR-101 mimics for 48 h, the total protein was isolated, collected, and measured by the BCA protein assay kit (Sigma-Aldrich). Proteins were separated by 10% sodium dodecyl sulfate-polyacrylamide gel electrophoresis gels and then transferred onto polyvinylidene fluoride membranes (0.45 μm; Sigma-Aldrich). The membranes were blocked with 5% nonfat milk in TBS containing 0.1% Tween 20 at 37°C for 2 h and incubated with primary antibodies against TGF-βR1 and β-actin (Cell Signaling Technology, Beverly, MA, USA) at 4°C overnight. The membranes were washed and probed with rabbit anti-mouse secondary antibody coupled with horseradish peroxidase (Sigma-Aldrich). The bands were developed by an enhanced chemiluminescence kit (Santa Cruz Biotechnology, Santa Cruz, CA, USA). Signals were detected by a Phosphor Imager (Storm 860 Version 4.0; Molecular Dynamics, Sunnyvale, CA, USA).

Tube Formation Assay

Tube formation assay was conducted to evaluate angiogenesis. After OSCC cells were transfected with miR-NC mimics, miR-101, or miR-101 + TGF-βR1 in the absence or presence of 100 ng/ml TGF-β1 for 48 h, the conditioned media were harvested. Subsequently, 1×10^5 human umbilical cord endothelial cells (HUVECs) were seeded in 48-well plates coated with Matrigel (BD Biosciences; 200 μl/well). After 24 h of incubation with the above conditioned media, the tube formation of the HUVECs was assessed with a phase-contrast microscope (Carl-Zeiss). The numbers of tubule and branch points were calculated using Image-Pro Plus software (Media Cybernetics Inc., Rockville, MD, USA).

Immunohistochemistry (IHC) Assay

The streptavidin–peroxidase method was employed to detect the TGF-βR1 levels in the OSCC and noncancerous tissue samples. The formalin-fixed and paraffin-embedded tissues were nonserially sectioned, treated with 3% H_2O_2, incubated in 5% goat antiserum, and treated with a primary antibody against TGF-βR1 overnight, followed by a biotin-labeled secondary antibody. Streptavidin–peroxidase complex was added, and the sections were stained with 3,3′-diaminobenzidine (Maixin Biotech., Fuzhou, China) prior to microscopic observation.

Statistical Analysis

Statistical analyses were performed using SPSS 11.5 software (SPSS Inc., Chicago, IL, USA). Data were from three independent experiments and presented as the mean ± standard deviation (SD). One-way analysis of variance (ANOVA) or Student's t-test was used to examine the differences between groups. Pearson correlation analysis was conducted to compare groups with high or low levels of miR-101 or TGF-βR1. A value of $p < 0.05$ was considered statistically significant.

RESULTS

Correlation Between miR-101 and TGF-βR1 Expression in OSCC Tissues and Cells

To investigate the potential roles of miR-101 in OSCC, we first detected the miR-101 levels in the OSCC tissues and cells. As shown in Figure 1A, miR-101 expression was downregulated in the OSCC tissues compared with that in the noncancerous samples. The 5-year overall survival rate of patients with high miR-101 levels was higher
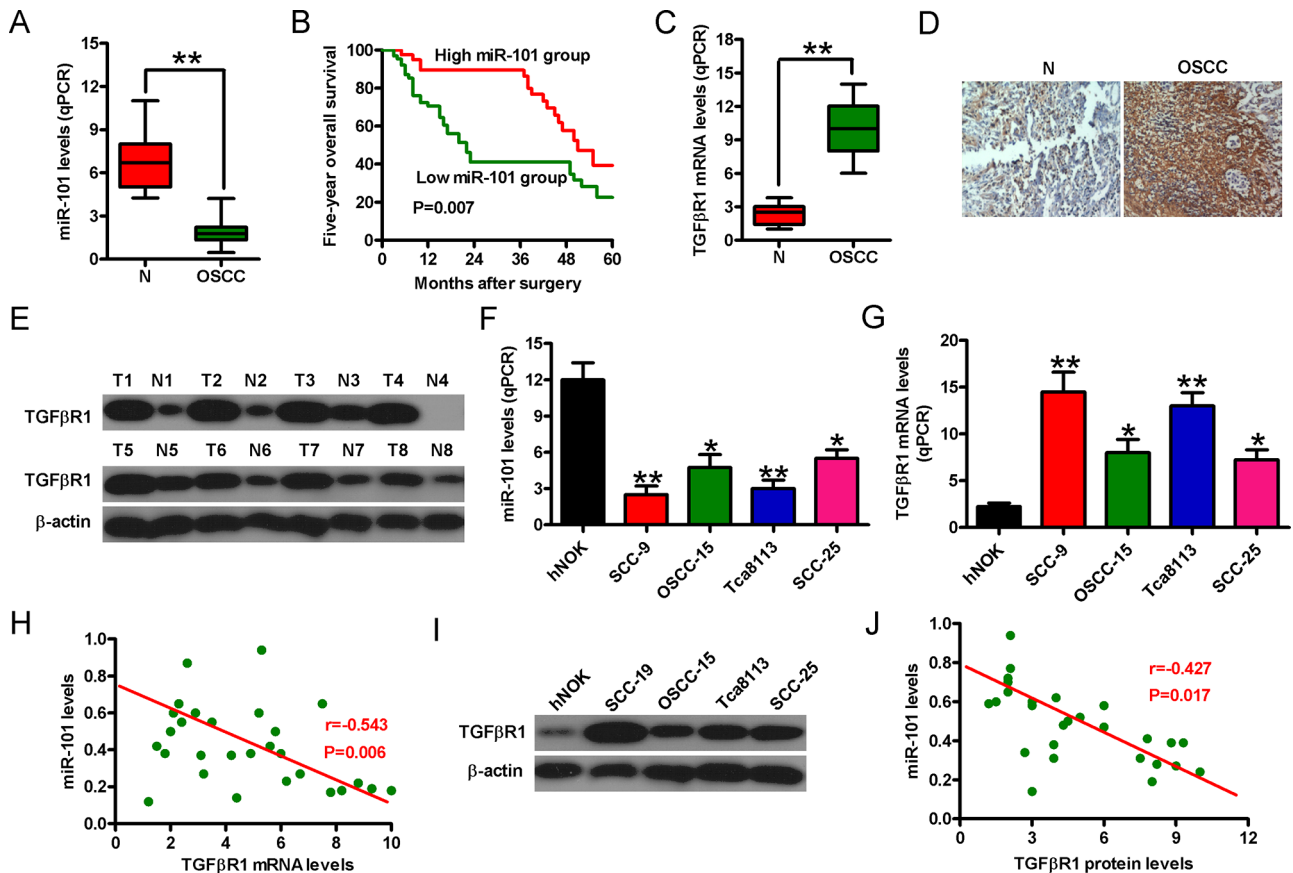
Figure 1. Negative correlation between microRNA-101 (miR-101) and transforming growth factor-β receptor 1 (TGF-βR1) expression in the oral squamous cell carcinoma (OSCC) tissues and cells. (A) Quantitative real-time polymerase chain reaction (qPCR) analysis of miR-101 levels in the OSCC tissues and adjacent noncancerous specimens ($n = 30$). U6 was used as the endogenous control. (B) Five-year overall survival rate of patients with high and low miR-101 levels. (C) TGF-βR1 mRNA expression was detected by qPCR assay in the OSCC tissues and adjacent noncancerous specimens. Glyceraldehyde-3-phosphate dehydrogenase (GAPDH) was used as the endogenous control. (D) Immunohistochemistry (IHC) assay was conducted to assess the levels of TGF-βR1 in the OSCC tissues and adjacent noncancerous specimens. (E) Western blot analysis of TGF-βR1 protein expression in the OSCC tissues and adjacent noncancerous specimens. β-Actin was used as the endogenous control. qPCR analyses of miR-101 (F) and TGF-βR1 mRNA (G) levels in the OSCC cells and human normal oral keratinocyte (hNOK) cells. (H) Negative correlation between the expression of TGF-βR1 mRNA and miR-101 in the OSCC cells ($r = -0.543$, $p = 0.006$). (I) Protein expression of TGF-βR1 in the OSCC cells and hNOK cells. (J) Negative correlation between TGF-βR1 protein levels and miR-101 in the OSCC cells ($r = -0.427$, $p = 0.017$). Data are shown as the mean ± standard deviation (SD) of three separate experiments. *$p < 0.05$ versus hNOK group; **$p < 0.01$ versus N and hNOK groups. N, noncancerous tissue specimen; T, tumor.

than that of those with low miR-101 levels (Fig. 1B). We performed qPCR, IHC, and Western blot assays to analyze TGF-βR1 expression in the OSCC tissues and adjacent nontumor tissues. TGF-βR1 mRNA was notably upregulated in the OSCC tissues compared with that in the adjacent nontumor tissues (Fig. 1C). IHC assay results revealed higher levels of TGF-βR1 in the OSCC tissues than in the normal specimens (Fig. 1D). Western blot analyses also confirmed that TGF-βR1 protein levels were higher in the cancer tissues than in the normal specimens (Fig. 1E). Additionally, miR-101 expression in the OSCC cell lines (i.e., Tca8113, OSCC-15, SCC-9, and SCC-25) was lower than that in the hNOK cells. However, the TGF-βR1 mRNA levels showed the opposite tendency (Fig. 1F and G). Spearman's correlation analysis further confirmed that TGF-βR1 mRNA expression exhibited a remarkably negative correlation with miR-101 levels ($r = -0.543$, $p = 0.006$) (Fig. 1H). As depicted in Figure 1I, the protein expression of TGF-βR1 in the OSCC cells was higher than that in the hNOK cells. The TGF-βR1 protein expression also presented a significantly negative correlation with miR-101 level in the OSCC cells ($r = -0.427$, $p = 0.017$) (Fig. 1J). The SCC-9 and Tca8113 cell lines were selected for further study because of their low miR-101 levels and high TGF-βR1 expression. These results indicated that miR-101 expression was negatively associated with TGF-βR1 level in OSCC.

miR-101 Directly Targeted TGF-βR1 in OSCC Cells

We then searched for the candidate target genes of miR-101 using the publicly available databases, such as TargetScan, miRBase, and miRanda (Fig. 2A). We identified a complementary region of miR-101 in the 3′-untranslated region (3′-UTR) of TGF-βR1 (Fig. 2B). Dual-luciferase reporter assay results revealed that miR-101 suppressed the luciferase activity of the reporter plasmid with TGF-βR1-3′-UTR-WT but did not inhibit that of a reporter plasmid fused to TGF-βR1-3′-UTR-MUT in the SCC-9 and Tca8113 cells (Fig. 2C and D). Meanwhile, qPCR and Western blot analyses showed that miR-101 reduced TGF-βR1 mRNA and protein expression in the SCC-9 and Tca8113 cells (Fig. 2E and F). These findings suggested that TGF-βR1 was a direct target of miR-101 in OSCC cells.

miR-101 Inhibited TGF-β1-Induced OSCC Cell Proliferation and Apoptosis Resistance by Targeting TGF-βR1

We explored whether TGF-βR1 is a functional target of miR-101 in the OSCC cells. SCC-9 and Tca8113 cells were transfected with miR-101, miR-NC, or miR-101 + TGF-βR1-expressing plasmid in the absence or presence of TGF-β1. EdU assay showed that viability decreased in the miR-101-transfected cells compared with that in the

miR-NC-treated cells, which was attenuated by TGF-βR1 overexpression in the basal and TGF-β1 groups (Fig. 3A and B). TGF-β1 stimulation markedly enhanced OSCC cell viability compared with basal treatment (Fig. 3A and B). Colony formation assay further confirmed the inhibitory effect of miR-101 on TGF-β1-induced cell proliferation. Compared with the basal group, the reduction in cell proliferation by miR-101 was more obvious in the TGF-β1-treated cells, which was reversed by TGF-βR1 overexpression (Fig. 3C and D). Moreover, flow cytometry and caspase 3 activity assays indicated that miR-101 reduced TGF-β1-decreased SCC-9 and Tca8113 cell apoptosis, which was abolished by TGF-βR1 overexpression (Fig. 3E and F). Our data showed that miR-101 abated TGF-β1-elicited proliferation and apoptosis resistance by targeting TGF-βR1 in the OSCC cells.

Overexpression of TGF-βR1 Counteracted the Suppressive Effects of miR-101 on the TGF-β1-Induced Migration and Invasion of OSCC Cells

We determined whether miR-101 hampers TGF-β1-induced migration and invasion of OSCC cells by targeting TGF-βR1. As shown in Figure 4A and B, miR-101 hindered the TGF-β1-induced migration of SCC-9 and Tca8113 cells, which was counteracted by TGF-βR1
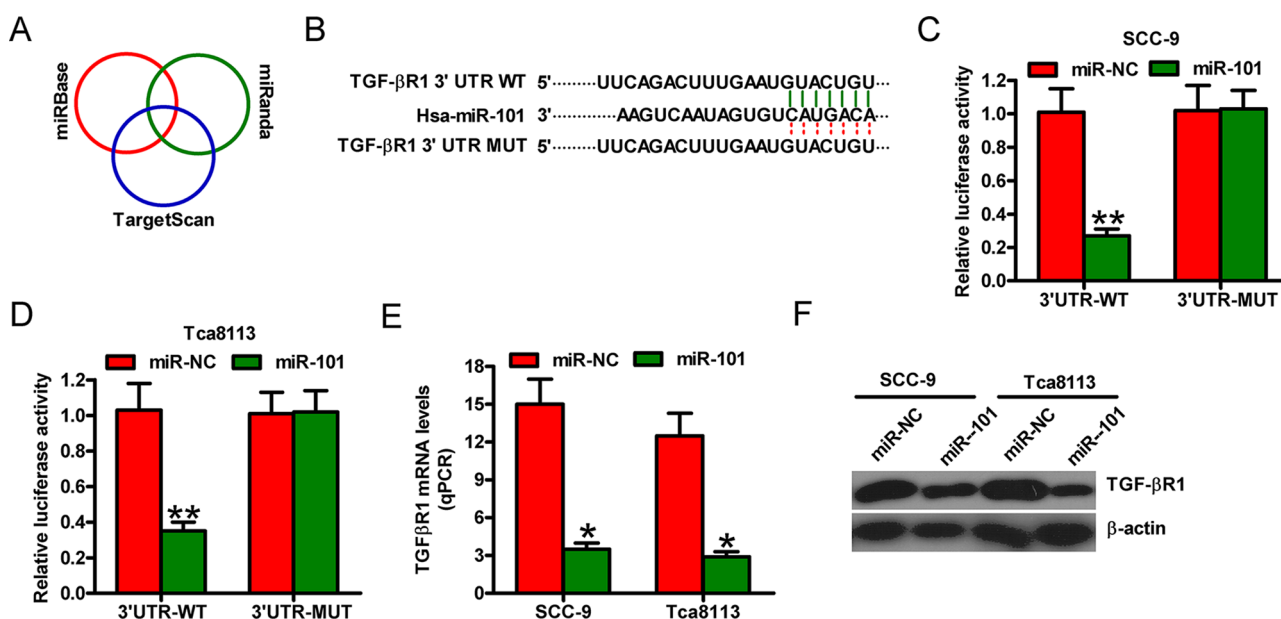

Figure 2. TGF-βR1 is a direct target of miR-101. (A) Prediction of the potential targets of miR-101 by integrating the results of three algorithms (TargetScan, miRBase, and miRanda). (B) The 3′-untranslated region (3′-UTR) of TGF-βR1 was predicted to contain a complementary region of miR-101 seed sequences. (C, D) Luciferase reporter plasmids harboring the WT or MUT 3′-UTR of TGF-βR1 were cotransfected with miR-NC or miR-101 mimics into the SCC-9 or Tca8113 cells. Luciferase reporter assays were performed at 24 h after cotransfection. The normalized luciferase activity in the group (miR-NC + the empty plasmid) was set to 1. The (E) mRNA and (F) protein levels of TGF-βR1 were determined by qPCR and Western blot assays in SCC-9 and Tca8113 cells transfected with miR-NC or miR-101. Data are presented as the mean ± SD of three replicates. *$p < 0.05$ versus miR-NC group; **$p < 0.01$ versus miR-NC group. MUT, mutate; NC, negative control; WT, wild type.
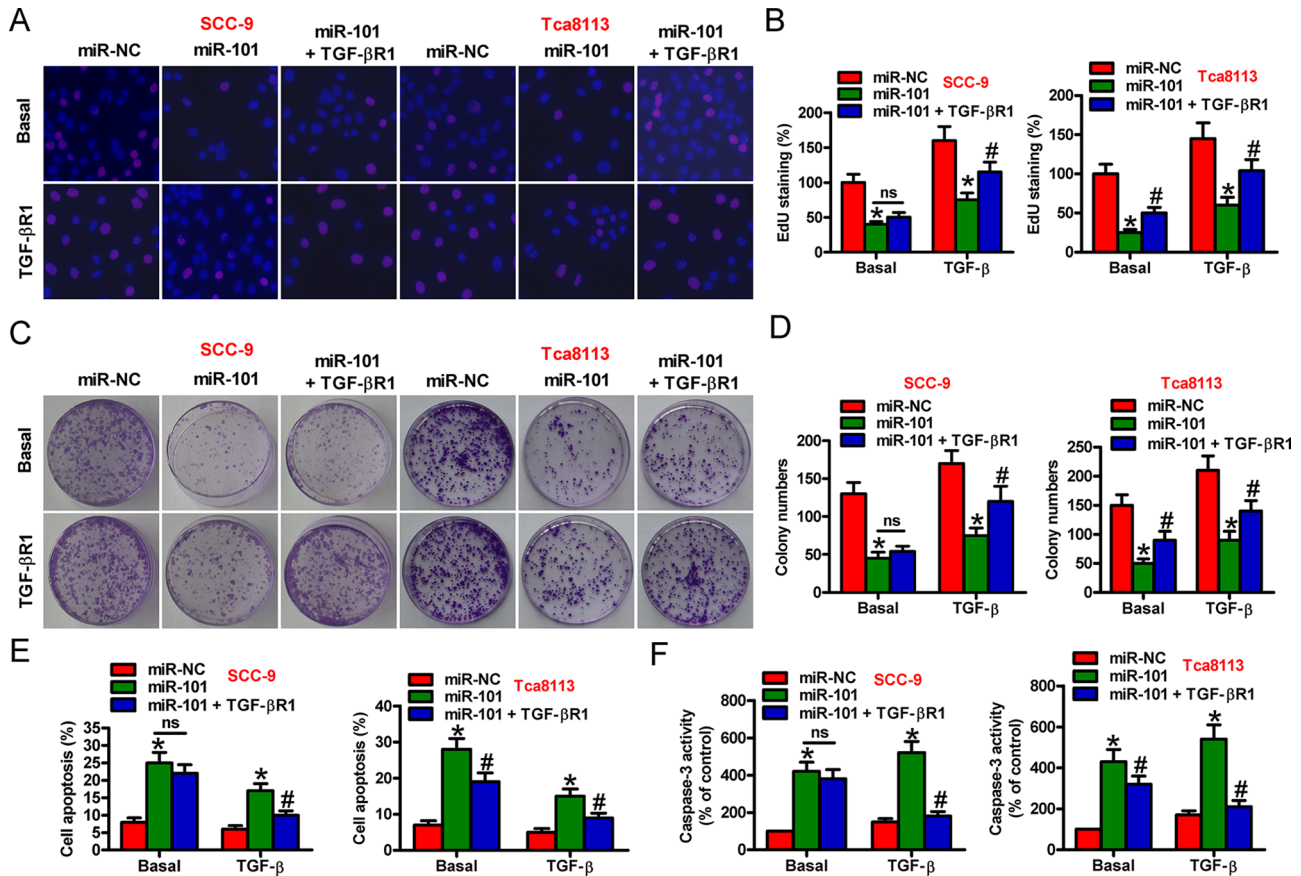
Figure 3. Suppression of TGF-β1-induced proliferation and apoptosis resistance by miR-101 was mediated by TGF-βR1 in OSCC cells. SCC-9 and Tca8113 cells were transfected with miR-NC, miR-101, or miR-101 + TGF-βR1-expressing plasmid in the absence or presence of TGF-β1. (A) EdU assay was performed to evaluate cell proliferation. (B) Percentage of EdU-positive cells in (A). (C) Colony formation assay was conducted to assess cell proliferation. (D) The number of colonies in (C) was counted. (E) Flow cytometry assay was performed to detect the apoptotic cells. Apoptotic rate was calculated. (F) Caspase 3 activity was measured to reflect cell apoptosis. Data are expressed as the mean ± SD of three separate experiments. *$p < 0.05$ versus miR-NC group; #$p < 0.05$ versus miR-101 group. ns, not significant.

rescue. The TGF-β1-induced invasion of SCC-9 and Tca8113 cells was restrained by miR-101, which was ameliorated by TGF-βR1 overexpression (Fig. 4C and D). These results demonstrated that TGF-βR1 was a functional mediator of miR-101 in TGF-β1-induced OSCC cell motility.

miR-101 Suppressed TGF-b1-Stimulated OSCC Cell-Induced Angiogenesis by Targeting TGF-bR1

We probed whether miR-101 exerts prohibitive effects on OSCC cell-promoted angiogenesis. Tube formation assay was conducted to evaluate the effects of OSCC cells on angiogenesis. As shown in Figure 5A, miR-101 reduced the angiogenesis of HUVECs treated with the conditioned medium from the TGF-β1-stimulated OSCC cells, which was reversed by TGF-βR1 overexpression. Consistently, the numbers of tubules and branch points showed similar tendencies

(Fig. 5B). These data implied that miR-101 attenuated the proangiogenesis effects of TGF-β-treated OSCC cells by downregulating TGF-βR1.

DISCUSSION

In this study, we demonstrated that miR-101 functioned as a tumor suppressor in OSCC by targeting TGF-βR1. The key findings were as follows (Fig. 6). First, miR-101 was significantly underexpressed in the OSCC tissues and cell lines and functioned as an independent prognostic factor. Second, TGF-βR1 was a direct and functional target of miR-101 in OSCC. Third, miR-101 inhibited OSCC cell proliferation, migration, and invasion and proangiogenesis. Fourth, the repressive effects of miR-101 on the malignant phenotypes of OSCC were attenuated by TGF-βR1 rescue. These results suggested the potential prognostic roles of miR-101 in OSCC and indicated that miR-101 retarded OSCC by targeting TGF-βR1.
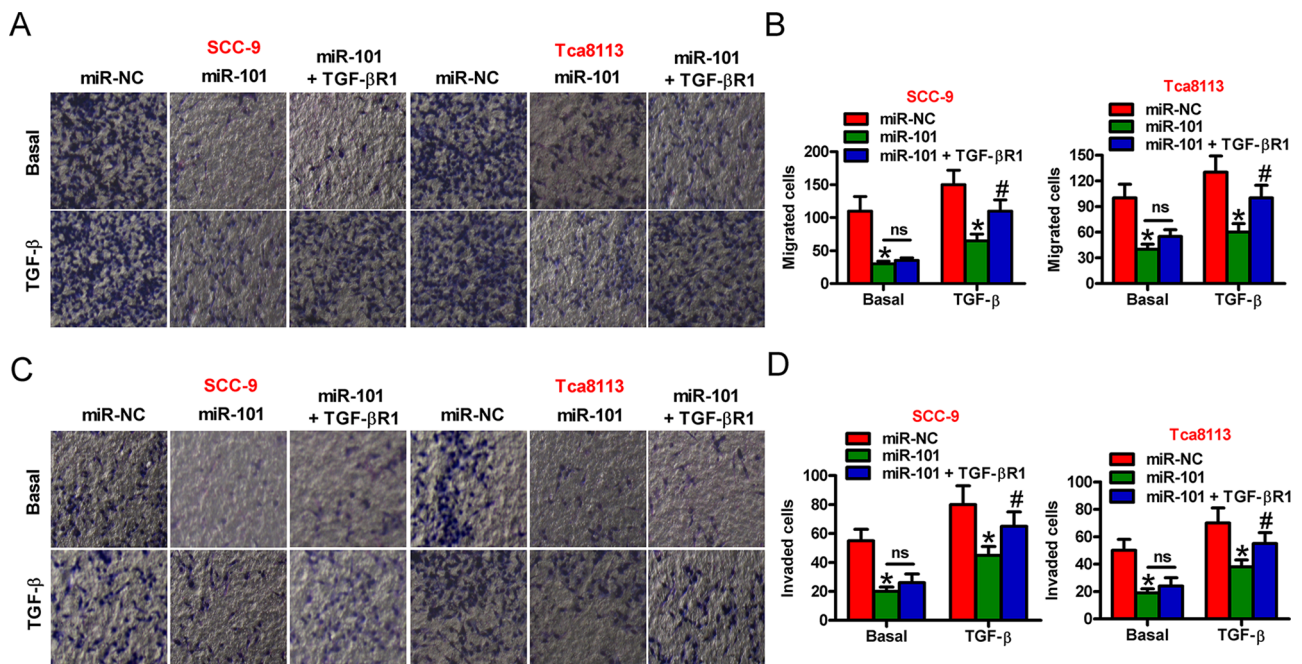
Figure 4. Inhibitory effects of miR-101 on TGF-β1-induced cell migration and invasion are executed by TGF-βR1 in OSCC cells. SCC-9 and Tca8113 cells were transfected with miR-NC, miR-101, or miR-101 + TGF-βR1-expressing plasmid in the absence or presence of TGF-β1. (A) Migration assay was performed to assess cell motility. (B) Migrated cells in (A) were measured. (C) Cell invasion was evaluated by Transwell assays. (D) The numbers of invaded cells in (C) were calculated. Data are shown as the mean ± SD of three separate experiments. $*p < 0.05$ versus miR-NC group; $\#p < 0.05$ versus miR-101 group. ns, not significant.

miRNAs play critical roles in the regulation of cell proliferation, invasion, and migration. miRNA dysregulation is involved in the initiation and progression of human cancers[11,12]. As a tumor-suppressive miRNA, miR-101 has been reported to be downregulated, and it suppresses the proliferation and colony formation ability of liver, breast, and colorectal cancer cells[14]. However, the expression of miR-101 in OSCC has rarely been identified. In this work, we demonstrated that miR-101 was poorly expressed in the OSCC tissue samples and cell lines. In accordance with other studies[20], we illuminated that miR-101 abolished OSCC cell proliferation and colony formation. miR-101 targets multiple effectors to repress the metastasis of malignancies[16,19]. Herein, we elucidated that miR-101 reduced OSCC cell migration and invasion. Although the evidence highlighted the important roles of miR-101 in oral tongue squamous cell carcinoma, the underlying mechanism by which miR-101 suppresses OSCC remains unclear. Hui et al.[21] showed that miR-101 abates OSCC growth and metastasis by targeting CXCR7. Zhao et al.[22] confirmed that miR-101 hampers hypoxia-caused cardiac fibrosis by targeting TGF-βR1 in fibroblasts. The relevance of TGF-βR1 to tumor progression has been studied in several human cancers[24]. Multiple components in the TGF-β signaling pathway have already been characterized as targets of miRNAs[25,26]. Recent studies have indicated that miR-101 attenuates the TGF-β signaling pathway, either by inhibiting the expression of TGFβ1 or by targeting TGF-βR1[22]. However, whether miR-101 targets TGF-βR1 to reduce OSCC remains unclear. Therefore, we chose TGF-βR1, one target of miRNA-101, as the research objective in OSCC. In the present study, TGF-βR1 was identified as a direct target of miR-101 in OSCC. miR-101 reduced the TGF-β1-increased OSCC cell proliferation, apoptosis resistance, migration, and invasion. However, this reduction was reversed by the ectopic expression of TGF-βR1, indicating that the inhibitory effects of miR-101 on OSCC were partly mediated by TGF-βR1.

Metastasis is a pathological feature in neoplasia with abnormal developmental and morphogenetic pathways, such as TGF-β and growth factor signaling[27]. The elevation of TGF-β promotes the malignant progression of cancers[28,29]. TGF-β exerts a procarcinogenesis effect by binding to two membrane serine/threonine kinase receptors, termed TGF-β type II receptor (TGF-βRII) and TGF-β type I receptor [TGFβ-R1; also termed activin-like kinase 5 (ALK5)][30]. Smads act as well-conserved components in the TGF-β family signal transduction pathway and further regulate the expression of a wide variety of oncogenes[31-33]. Here we observed that miR-101 inhibited
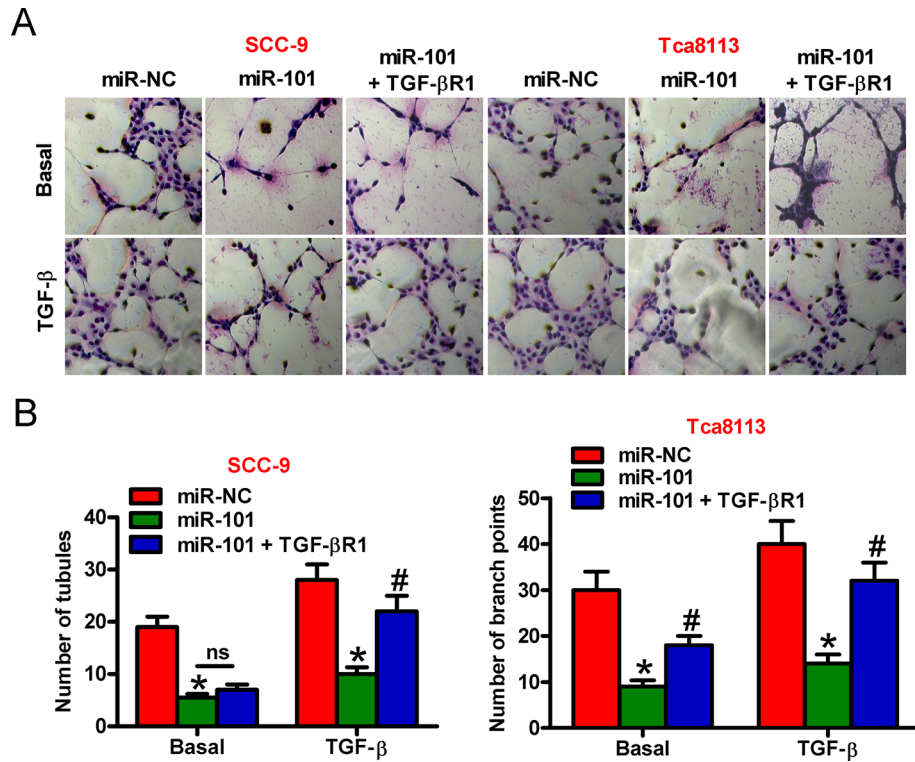
Figure 5. miR-101 repressed the proangiogenesis ability of TGF-β1-treated OSCC cells by targeting TGF-βR1. SCC-9 and Tca8113 cells were transfected with miR-NC, miR-101, or miR-101 + TGF-βR1-expressing plasmid in the absence or presence of TGF-β1. The collected conditioned medium of each group was added into human umbilical cord endothelial cells (HUVECs). (A) Tube formation assay was conducted to evaluate the angiogenesis of HUVECs. (B) The numbers of tubules and branch points in (A) were calculated. Data are shown as the mean ± SD of three separate experiments. *$p < 0.05$ versus miR-NC group; #$p < 0.05$ versus miR-101 group. ns, not significant.
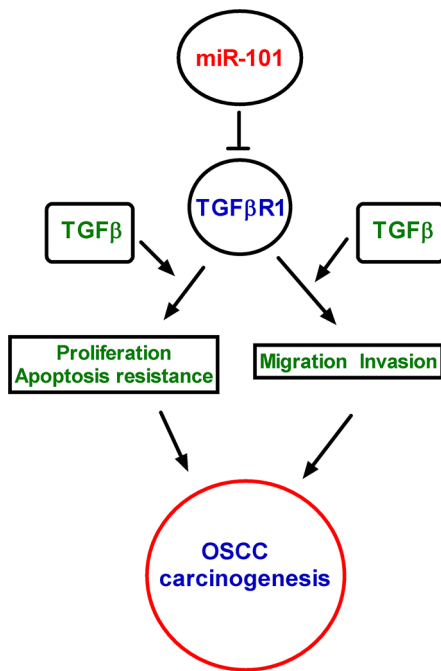

Figure 6. Schematic summaries of the relationship of miR-101, TGF-β1, TGF-βR1, and OSCC cell proliferation, migration, invasion, and angiogenesis.

the TGF-β1-induced migration and invasion of OSCC cells by targeting TGFβ-R1, suggesting TGFβ-R1 as a functional mediator of miR-101 in TGF-β1-facilitated OSCC cell motility.

Inappropriate angiogenic signaling leads to aberrant neovascularization, which contributes to cancers[34]. Angiogenesis is a complex procedure by which capillaries sprout from vessels and allow tumor cells to metastasize to distant sites from primary lesions[35]. Jin et al. reported that TGF-β1 signaling promoted hematopoietic stem cells to express Jagged1 and VEGF-A, which were conducive to angiogenesis[36]. The present study investigated the role of miR-101 in the regulation of the proangiogenetic ability of TGF-β1-induced OSCC cells. miR-101 repressed OSCC cell-induced angiogenesis, which was counteracted by TGFβ-R1 overexpression. This result implied that TGFβ-R1 mediated the inhibitory effects of miR-101 on the proangiogenesis of TGF-β1-stimulated OSCC cells.

This study has several limitations. We only illuminated the repressive effects of miR-101 on OSCC malignancies but did not further identify the underlying mechanisms. In future studies, we will investigate the molecular mechanisms by which miR-101 affected OSCC evolution, such as epithelial–mesenchymal transition.

In summary, we found that miR-101 was weakly expressed in the OSCC tissues and cell lines and identified as an independent prognostic factor. miR-101 significantly abolished TGF-β1-augmented proliferation, migration, apoptosis resistance, and proangiogenesis of OSCC cells. miR-101 directly targeted TGF-βR1 in the OSCC cells. The inhibitory effects of miR-101 on the malignant phenotypes of OSCC were attenuated by the overexpression of TGF-βR1. These findings provide new insight into the potential prognostic role of miR-101 in OSCC and reveal that miR-101 targets TGF-βR1 to reduce OSCC carcinogenesis.

REFERENCES

1. Siegel RL, Miller KD, Jemal A. Cancer statistics, 2019. CA Cancer J Clin. 2019;69(1):7–34.

2. Chen W, Zheng R, Baade PD, Zhang S, Zeng H, Bray F, Jemal A, Yu XQ, He J. Cancer statistics in China, 2015. CA Cancer J Clin. 2016;66(2):115–32.

3. Miller KD, Nogueira L, Mariotto AB, Rowland JH, Yabroff KR, Alfano CM, Jemal A, Kramer JL, Siegel RL. Cancer treatment and survivorship statistics, 2019. CA Cancer J Clin. 2019;69(5):363–85.

4. Montagnani F, Fornaro L, Frumento P, Vivaldi C, Falcone A, Fioretto L. Multimodality treatment of locally advanced squamous cell carcinoma of the oesophagus: A comprehensive review and network meta-analysis. Crit Rev Oncol Hematol. 2017;114:24–32.

5. Ketabat F, Pundir M, Mohabatpour F, Lobanova L, Koutsopoulos S, Hadjiiski L, Chen X, Papagerakis P, Papagerakis S. Controlled drug delivery systems for oral cancer treatment—Current status and future perspectives. Pharmaceutics 2019;11(7).

6. Croce CM, Calin GA. miRNAs, cancer, and stem cell division. Cell 2005;122(1):6–7.

7. Calin GA, Croce CM. MicroRNA signatures in human cancers. Nat Rev Cancer 2006;6(11):857–66.

8. Esteller M. Non-coding RNAs in human disease. Nat Rev Genet. 2011;12(12):861–74.

9. Rupaimoole R, Slack FJ. MicroRNA therapeutics: Towards a new era for the management of cancer and other diseases. Nat Rev Drug Discov. 2017;16(3):203–22.

10. Jamali Z, Asl AN, Attaran R, Pournagiazar F, Ghertasi OS, Ahmadpour F. MicroRNAs as prognostic molecular signatures in human head and neck squamous cell carcinoma: A systematic review and meta-analysis. Oral Oncol. 2015;51(4):321–31.

11. Karatas OF, Oner M, Abay A, Diyapoglu A. MicroRNAs in human tongue squamous cell carcinoma: From pathogenesis to therapeutic implications. Oral Oncol. 2017;67:124–30.

12. Momen-Heravi F, Bala S. Emerging role of non-coding RNA in oral cancer. Cell Signal 2018;42:134–43.

13. Yu X, Li Z. MicroRNA expression and its implications for diagnosis and therapy of tongue squamous cell carcinoma. J Cell Mol Med. 2016;20(1):10–16.

14. Wang CZ, Deng F, Li H, Wang DD, Zhang W, Ding L, Tang JH. MiR-101: A potential therapeutic target of cancers. Am J Transl Res. 2018;10(11):3310–21.

15. Miao L, Wang L, Yuan H, Hang D, Zhu L, Du J, Zhu X, Li B, Wang R and Ma H, Chen N. MicroRNA-101 polymorphisms and risk of head and neck squamous cell carcinoma in a Chinese population. Tumour Biol. 2016;37(3):4169–74.

16. Chandra MK, Manvati S, Saini SK, Ponnusamy K, Agarwal G, Abraham SK, Bamezai R. ERK2–ZEB1–miR-101-1 axis contributes to epithelial–mesenchymal transition and cell migration in cancer. Cancer Lett. 2017;391:59–73.

17. Liu XY, Liu ZJ, He H, Zhang C, Wang YL. MicroRNA-101-3p suppresses cell proliferation, invasion and enhances chemotherapeutic sensitivity in salivary gland adenoid cystic carcinoma by targeting Pim-1. Am J Cancer Res. 2015;5(10):3015–29.

18. Cao K, Li J, Zhao Y, Wang Q, Zeng Q, He S, Yu L, Zhou J, Cao P. miR-101 inhibiting cell proliferation, migration and invasion in hepatocellular carcinoma through downregulating girdin. Mol Cells 2016;39(2):96–102.

19. Xiong WC, Han N, Wu N, Zhao KL, Han C, Wang HX, Ping GF, Zheng PF, Feng H, Qin L, He P. Interplay between long noncoding RNA ZEB1-AS1 and miR-101/ZEB1 axis regulates proliferation and migration of colorectal cancer cells. Am J Transl Res. 2018;10(2):605–17.

20. Wu B, Lei D, Wang L, Yang X, Jia S, Yang Z, Shan C, Yang X, Zhang C, Lu B. MiRNA-101 inhibits oral squamous-cell carcinoma growth and metastasis by targeting zinc finger E-box binding homeobox 1. Am J Cancer Res. 2016;6(6):1396–407.

21. Hui Y, Li Y, Jing Y, Feng JQ, Ding Y. miRNA-101 acts as a tumor suppressor in oral squamous cell carcinoma by targeting CX chemokine receptor 7. Am J Transl Res. 2016;8(11):4902–11.

22. Zhao X, Wang K, Liao Y, Zeng Q, Li Y, Hu F, Liu Y, Meng K, Qian C, Zhang Q, Guan H, Feng K, Zhou Y, Du Y, Chen Z. MicroRNA-101a inhibits cardiac fibrosis induced by hypoxia via targeting TGFbetaRI on cardiac fibroblasts. Cell Physiol Biochem. 2015;35(1):213–26.

23. Guan H, Dai Z, Ma Y, Wang Z, Liu X, Wang X. MicroRNA-101 inhibits cell proliferation and induces apoptosis by targeting EYA1 in breast cancer. Int J Mol Med. 2016;37(6):1643–51.

24. Jiang Y, Chen X, Tian W, Yin X, Wang J, Yang H. The role of TGF-beta1–miR-21–ROS pathway in bystander responses induced by irradiated non-small-cell lung cancer cells. Br J Cancer 2014;111(4):772–80.

25. Cheng CM, Shiah SG, Huang CC, Hsiao JR, Chang JY. Up-regulation of miR-455-5p by the TGF-beta–SMAD signalling axis promotes the proliferation of oral squamous cancer cells by targeting UBE2B. J Pathol. 2016;240(1):38–49.

26. Fang LL, Sun BF, Huang LR, Yuan HB, Zhang S, Chen J, Yu ZJ, Luo H. Potent inhibition of miR-34b on migration and invasion in metastatic prostate cancer cells by regulating the TGF-beta pathway. Int J Mol Sci. 2017;18(12).

27. Jensen DH, Dabelsteen E, Specht L, Fiehn AM, Therkildsen MH, Jonson L, Vikesaa J, Nielsen FC, von Buchwald C. Molecular profiling of tumour budding implicates TGFbeta-mediated epithelial–mesenchymal transition as a therapeutic target in oral squamous cell carcinoma. J Pathol. 2015;236(4):505–16.

28. Chen Y, Di C, Zhang X, Wang J, Wang F, Yan JF, Xu C, Zhang J, Zhang Q, Li H, Yang H, Zhang H. Transforming growth factor beta signaling pathway: A promising therapeutic target for cancer. J Cell Physiol. 2020;235(3):1903–14.

29. Batlle E, Massague J. Transforming growth factor-beta signaling in immunity and cancer. Immunity 2019;50(4):924–40.

30. Drabsch Y, Ten DP. TGF-beta signalling and its role in cancer progression and metastasis. Cancer Metastasis Rev. 2012;31(3–4):553–68.

31. Sun H, Miao C, Liu W, Qiao X, Yang W, Li L, Li C. TGF-beta1/TbetaRII/Smad3 signaling pathway promotes VEGF expression in oral squamous cell carcinoma tumor-associated macrophages. Biochem Biophys Res Commun. 2018;497(2):583–90.

32. Jiang X, Zhang Z, Song C, Deng H, Yang R, Zhou L, Sun Y, Zhang Q. Glaucocalyxin A reverses EMT and TGF-beta1-induced EMT by inhibiting TGF-beta1/Smad2/3 signaling pathway in osteosarcoma. Chem Biol Interact. 2019;307:158–66.

33. Derynck R, Zhang YE. Smad-dependent and Smad-independent pathways in TGF-beta family signalling. Nature 2003;425(6958):577–84.

34. Wang X, Abraham S, McKenzie J, Jeffs N, Swire M, Tripathi VB, Luhmann U, Lange C, Zhai Z, Arthur HM, Brainbridge J, Moss SE, Greenwood J. LRG1 promotes angiogenesis by modulating endothelial TGF-beta signalling. Nature 2013;499(7458):306–11.

35. Ferrari G, Cook BD, Terushkin V, Pintucci G, Mignatti P. Transforming growth factor-beta 1 (TGF-beta1) induces angiogenesis through vascular endothelial growth factor (VEGF)-mediated apoptosis. J Cell Physiol. 2009;219(2):449–58.

36. Jin X, Aimaiti Y, Chen Z, Wang W, Li D. Hepatic stellate cells promote angiogenesis via the TGF-beta1-Jagged1/VEGFA axis. Exp Cell Res. 2018;373(1–2):34–43.